Mon. Not. R. Astron. Soc. **372,** 1681–1691 (2006) doi:10.1111/j.1365-2966.2006.10985.x

What does the quasar luminosity function tell us about supermassive black hole evolution?

J. Stuart B. Wyithe[1⋆] and T. Padmanabhan[2⋆]

[1]*School of Physics, University of Melbourne, Parkville, Victoria, Australia*
[2]*Inter-University Centre for Astronomy and Astrophysics, Pune, India*

Accepted 2006 August 22. Received 2006 July 24; in original form 2006 March 13

ABSTRACT

In the local Universe, the masses of supermassive black holes (SMBH) appear to correlate with the physical properties of their hosts, including the mass of the dark matter halo. Using these clues as a starting point many studies have produced models that can explain phenomena like the quasar luminosity function. The shortcoming of this approach is that working models are not unique, and as a result it is not always clear what input physics is being constrained. Here we take a different approach. We identify critical parameters that describe the evolution of SMBHs at high redshift, and constrain their parameter space based on observations of high-redshift quasars from the Sloan Digital Sky Survey. We find that the luminosity function taken in isolation is somewhat limited in its ability to constrain SMBH evolution due to some strong degeneracies. This explains the presence in the literature of a range of equally successful models based on different physical hypotheses. Including the constraint of the local SMBH to halo mass ratio breaks some of the degeneracies, and our results suggest halo masses at $z \sim 4.8$ of $10^{12.5\pm0.3}\,M_\odot$ (with 90 per cent confidence), with an SMBH to halo mass ratio that decreases with time (>99 per cent). We also find a quasar luminosity to halo mass ratio that increases with halo mass (>99 per cent). These features need to be incorporated in all successful models of SMBH evolution. On the other hand current observations do not permit any conclusions regarding the evolution of quasar lifetime, or the SMBH occupation fraction in dark matter haloes.

Key words: galaxies: formation – cosmology: theory.

1 INTRODUCTION

The Sloan Digital Sky Survey (SDSS) has discovered luminous quasars at redshifts as high as $z \sim 6.4$, that is, when the Universe was only a billion years old. The supermassive black holes (SMBH) powering these quasars have been estimated to have masses of $\sim 10^9\,M_\odot$. There is evidence that SMBHs contained a larger fraction of the host bulge mass at high redshift (Merloni, Rudnick & Di Matteo 2004; Peng et al. 2006; Shields et al. 2006). There are, however, several other questions regarding the galaxies that host these high-redshift quasars, and the physics that govern their evolution that have remained largely unanswered. Traditionally, investigation of the evolution of high-redshift quasars has revolved around construction of models for the luminosity function which can be compared with observation. In this way successful models can be labelled as possible candidates to explain the formation and evolution of the quasars. An equally valuable, though a rarer approach is to rule out potential models because they are unable provide an explanation for the observed population. This approach is important because while a successful model can only suggest a mechanism as one possibility, a model which does not reproduce an observed phenomena may be definitely ruled out.

Many successful models have been produced to explain the high-redshift luminosity function (e.g. Haehnelt, Natarajan & Rees 1998; Haiman & Loeb 1998; Kauffmann & Haehnelt 2000; Di Matteo et al. 2003; Volonteri, Haardt & Madau 2003; Wyithe & Loeb 2003). Some authors advocate the view that the simpler a model the better because simple models can more clearly elucidate the important underlying physics. Others would argue that more detailed numerical models that attempt to capture more of the complex non-linear processes involved offer a more realistic and reliable description. Models for the luminosity function, therefore, take a variety of forms and complexity. These range from analytic models in which simple physical prescriptions are combined with the Press–Schechter (PS) (1974) mass function and merger rates; to more complex semi-analytic models with merger trees and parametrized laws to describe physical processes; through to numerical simulations with quasar activity included through a semi-analytic prescription. The published

⋆E-mails: swyithe@physics.unimelb.edu.au (JSBW); nabhan@iucaa.ernet.in (TP)

models of all types are broadly successful in their reproduction of high-redshift number counts. In general this is because if one adds the number of free parameters to the number of physical assumptions, then one gets a number of parameters that is comparable to or smaller than the effective number of constraints (which in practice includes only the slope of the luminosity function and the evolution of slope with redshift, in addition to the density normalization).

In this paper we highlight the fact that many different models are able to reproduce the data on the high-redshift quasar luminosity function, and note that this implies some degeneracy among input physical parameters or mechanisms. Indeed, one such degeneracy was pointed out in an early model for high-redshift quasar evolution (Haehnelt et al. 1998). Assuming that quasar number counts trace the number of dark matter halo hosts, Haehnelt et al. (1998) found that the luminosity function at $z > 2$ could be equally well described using a constant SMBH to halo mass ratio combined with a constant lifetime; or using a mass dependent SMBH to halo mass ratio combined with a lifetime that decreased towards high redshift. The latter possibility is expected from a feedback scenario for SMBH growth (Silk & Rees 1998). The degeneracy described above would imply that one cannot obtain strong evidence for feedback using only the high-redshift luminosity function data. More generally, these types of degeneracies mean that it is difficult to know which physical features of the various models are being constrained by the data. Indeed we would like to know whether it is possible to conclude anything from published models other than the fact that the population of high-redshift quasars can be reconciled with the Lambda cold dark matter cosmology.

One feature that all models have in common is that they are based on the density and evolution of the dark matter halo population. In semi-analytic models this population is generally modelled according to the PS (1974) mass function (with extensions). Similar results are obtained in cases where cosmological *N*-body codes are used because the PS mass function provides an accurate reflection of simulations over the mass-range of interest. In common with previous work, we use the PS mass function as a starting point from which the quasar population is generated. However, we do not attempt to model physical processes such as SMBH growth and feedback, etc., as is done in traditional semi-analytic modelling. Instead we take the more general approach of applying arbitrary parametrizations of processes like the evolution of quasar lifetime, and the evolution of the relation between SMBH mass, halo mass and redshift. While it is true that we assign free parameters to describe processes that we do not understand, the procedure for finding *sets* of these parameters which satisfy the data in a statistical sense is fundamentally different from the usual procedure of semi-analytic modelling which aims to find a single successful model. We are interested in the full range of allowed parameters as well as which sets of parameters can be excluded, rather than in a single set of parameters that is able to describe the data. In this way we hope to provide guidance for future attempts to build physical models of SMBH evolution.

The optical quasar luminosity function shows a peak in its evolution at $z \sim 2$–3. At higher redshifts the quasar population grows with time, and it is natural to relate the rise of the quasar population to the rise of the dark matter halo population (e.g. Haehnelt et al. 1998; Haiman & Loeb 1998; Volonteri et al. 2003; Wyithe & Loeb 2003). However, near a redshift of $z \sim 2$–3 the non-linear mass scale moves from galactic scale to cluster scale. It is thought that the rapid fall in the density of bright quasars below $z \sim 2$ is due to a combination of a dwindling supply of cold gas at late times (Kauffmann & Haehnelt 2000) with an injection of feedback from the quasars into the surrounding intergalactic medium that prevents further gas accretion on to collapsing systems (Scannapieco & Oh 2004). Following the peak of quasar evolution one can no longer relate the growth of the quasar (or galaxy) population directly to that of the dark matter halo population in any direct or model independent way. For these reasons we restrict our attention to quasars at redshifts beyond $z \sim 3.7$, where we can relate the evolution in the quasar luminosity function directly to evolution of the PS (1974) mass function.

In Section 2 we introduce our parametrization of SMBH/quasar evolution, discuss the relation of these parameters to quasar observables, and present our method of parameter estimation as well as our choice of prior probabilities for the different variables. Our approach is an extension of the formalism described in Wyithe & Padmanabhan (2006, hereafter Paper I). In Sections 3 and 4 we describe the constraints that the available data impose on physical and model parameters. The effects of scatter in the relation between quasar luminosity and halo mass and of the choice of parametrization and prior probabilities are discussed in Sections 5 and 6. Finally, we compare some simple physical models with our derived constraints (Section 7) before summarizing our results in Section 8. Throughout the paper we adopt the set of cosmological parameters determined by the *Wilkinson Microwave Anisotropy Probe* (*WMAP*; Spergel et al. 2003), namely mass density parameters of $\Omega_{\rm m} = 0.27$ in matter, $\Omega_{\rm b} = 0.044$ in baryons, $\Omega_\Lambda = 0.73$ in a cosmological constant, and a Hubble constant of $H_0 = 71\,{\rm km\,s^{-1}\,Mpc^{-1}}$. For the primordial power-spectrum of density fluctuations, we adopt a power-law slope $n = 1$, and the fitting formula to the exact transfer function of Bardeen et al. (1986).

2 MODEL PARAMETERS AND CONSTRAINTS

2.1 Parameters

In this section we introduce our parametrization of SMBH evolution. Our aim is to describe a parametrized, rather than a physical, model of SMBH evolution. We do not attempt to assign values for these parameters in order to represent a particular physical theory. Rather our goal is to consider all values so as to elucidate the acceptable range of parameter values as well as any degeneracies. The parametrization chosen provides a general set of models within which the various different possible physical models are contained. Therefore by using this set of models to constrain the allowed values for these parameters, we may determine which physical processes can be unambiguously extracted from the available data.

We define halo mass M to be the mass of a halo hosting a quasar with a luminosity $\mathcal{M}_{1450} = -26.7$ at $z = 4.8$. The relation between quasar luminosity L and halo mass M may have a mass dependence and a redshift dependence in addition to a normalization (L_0/M_0). We parametrize this dependence using two indices δ and γ as

$$\frac{L(z)}{L_0} = \left(\frac{M}{M_0}\right)^{\delta} (1+z)^{\gamma}. \quad (1)$$

Equation (1) is assumed to be valid at high redshift ($z \sim 4.8$), where we consider the evolution of the quasar population. Similarly we may also parametrize the dependence of SMBH mass on halo mass using the same parameters

$$\frac{M_{\rm bh}(z)}{M_{\rm bh,0}} = \left(\frac{M}{M_0}\right)^{\delta} (1+z)^{\gamma}. \quad (2)$$

We assume equation (2) to be valid at all redshifts. The combination of equations (1) and (2) describes an implicit assumption that all SMBHs accrete at the same rate in high-redshift quasars. However,

we allow the accretion rate to vary arbitrarily at low redshift where it does not enter our analysis.

The PS (1974) mass function $n(M, z)$, [with the modification of Sheth & Torman (2002) that will be adopted throughout our discussion] yields the number density $N(>M(z), z)$ of dark matter haloes above some mass $M(z)$ at redshift z. In this paper we assume that a fraction (equal to the quasar duty cycle) of SMBHs are powering quasars at any given instant, and that SMBHs reside in a fraction ϵ of such dark matter haloes. We further assume that the duty cycle can be approximated by the quasar lifetime divided by the Hubble time. The observed number density of quasars is therefore given by the product of two factors:

$$N(< \mathcal{M}_{1450}) = N(> M(z), z)\tau, \tag{3}$$

where

$$\tau \equiv \epsilon \min\left\{\frac{t_{\rm q}}{H^{-1}(z)}, 1\right\}, \tag{4}$$

$t_{\rm q}$ is the (unknown) quasar lifetime and $H^{-1}(z)$ is the Hubble time (see e.g. Efstathiou & Rees 1998). Note that this definition does not necessarily associate quasar activity with processes such as the halo merger or halo formation rate.

Our fourth parameter is introduced via the z dependence of $t_{\rm q}$. While ϵ could also change with z due to various effects (dust obscuration, beaming angle, etc.), we expect the dominant contribution to evolution in τ to come from $t_{\rm q}$. Nevertheless, we allow for growth of ϵ with time. The evolution of τ can be parametrized by

$$\frac{\tau(z)}{\tau_0} = (1+z)^{\alpha}. \tag{5}$$

The parameters α, γ and δ, in addition to $\log_{10} M$ therefore govern the evolution of SMBHs. In this paper our goal is to constrain the allowed values of these parameters using observations of high-redshift quasars. (Note that the model described above assumes an arbitrarily chosen a power-law parametrization. The effect of modifying this choice is investigated in Section 6.)

2.2 Observational constraints

There are three observational constraints which we will use to identify the allowed range of parameters governing the evolution of SMBHs (α, δ and γ) as well as halo mass M. Let us discuss key observations that constrain these.

First, observations of high-redshift quasars (Fan et al. 2001, 2003, 2004) reveal an exponential decline in the quasar population with redshift of the form

$$\Psi(\mathcal{M}_{1450} < -26.7, z) \propto 10^{B_{\rm obs} z}, \tag{6}$$

suggesting approximate constancy of B. As a measure of the rate at which luminous quasars appear, we therefore use the exponential slope (B) of $\tau N(>M(z), z)$, which according to the above parametrization is defined as

$$B = 0.434\frac{\alpha}{1+z} + \frac{\partial \log_{10} N(> M, z)}{\partial z} - \frac{0.434}{(1+z)}\frac{\gamma}{\delta}\frac{{\rm d}\log_{10} N(> M, z)}{{\rm d}\log_{10} M}. \tag{7}$$

Secondly, observations of high-redshift quasars (Fan et al. 2001) also reveal a power-law decline in the density of quasars per unit luminosity as a function of luminosity of the form

$$\frac{{\rm d}\Psi}{{\rm d}L} \propto L^{\beta}. \tag{8}$$

As a measure of the relative numbers of quasars with different luminosities at a single redshift we use the power-law slope of the halo mass function $n(M, z) = {\rm d}N(>M)/{\rm d}M$

$$\beta = \frac{1}{\delta}\frac{{\rm d}\log_{10}(n)}{{\rm d}\log_{10}(M)}. \tag{9}$$

The factor of $1/\delta$ accounts for the non-linear relation between luminosity and halo mass.

Thirdly, the ratio of SMBH to host dark matter halo mass is determined locally. Given an SMBH to host dark matter halo mass ratio $R(M, z)$ at high redshift, we can compute an extrapolated ratio at $z = 0$ for haloes of mass $M_0 = 10^{12}\,{\rm M}_{\odot}$ using the parameters δ and γ:

$$R_0(10^{12}\,{\rm M}_{\odot}, 0) = R\,(M, z)\left(\frac{M}{10^{12}\,{\rm M}_{\odot}}\right)^{1-\delta}(1+z)^{-\gamma}. \tag{10}$$

Here, we have assumed that $L \propto M_{\rm bh}$ at high redshift where the SDSS quasars are observed (equation 1). However, the local SMBH masses and therefore the value of R_0 are measured directly. Equation (10) therefore does not contain any assumption regarding the evolution of the accretion rate towards low redshift. If we estimate the SMBH mass powering the high-redshift quasars, then we can calculate $R(M, z)$ for a given value of host mass M and compare the extrapolated value of R_0 for haloes of $10^{12}\,{\rm M}_{\odot}$ at $z = 0$ with the observations. Equation (1) relates the quasar luminosity to the dark matter halo mass, and can therefore (as discussed in the introduction) only be applied at high redshift, prior to the decline in the quasar population. In contrast, we assume the functional form of the relation between SMBH and halo mass, which is the basis of equation (10), to be common at low and high redshift.

In this paper we assign Gaussian probabilities for the observed distributions of B, β and R_0. In Paper I, based on the data of Fan et al. (2001, 2003, 2004) we found that $B_{\rm obs}$ is well constrained with a mean $\bar{B} = -0.49$ and variance $\Delta B = 0.07$. Fan et al. (2001) find $\bar{\beta} = -2.58$ and $\Delta\beta = 0.23$. Ferrarese (2002) determines the ratio $M_{\rm bh}/M$ for $M = 10^{12}\,{\rm M}_{\odot}$ and finds a significant dependence on the assumed mass profile, with values ranging between $\log_{10} R_0 = -5$ (for an NFW profile) and $\log_{10} R_0 = -5.6$ (for an singular isothermal profile). Since the true profile is likely to lie between these extremes, we adopt a mean of $\log_{10} \bar{R}_0 = -5.3$ and a variance $\Delta\log_{10} R_0 = 0.3$.

2.3 A posteriori parameter estimation

From Bayes theorem, the joint a posteriori probability distribution for the parameters of interest (α, δ, γ and M) as well as σ_8 is

$$\left.\frac{{\rm d}^5 P}{{\rm d}\alpha\,{\rm d}\gamma\,{\rm d}\delta\,{\rm d}\log_{10} M\,{\rm d}\sigma_8}\right|_{\rm obs} \propto L_B L_{\beta} L_R \frac{{\rm d}P_{\rm prior}}{{\rm d}\gamma}\frac{{\rm d}P_{\rm prior}}{{\rm d}\alpha}\frac{{\rm d}P_{\rm prior,obs}}{{\rm d}\delta}\frac{{\rm d}P_{\rm prior}}{{\rm d}\log_{10} M}\frac{{\rm d}P_{\rm obs}}{{\rm d}\sigma_8}. \tag{11}$$

In what follows we will consider both the prior and observed constraints for δ, hence the designation $P_{\rm prior,obs}$ in equation (11). Since σ_8 has an observed distribution, we may marginalize over its dependence:

$$\left.\frac{{\rm d}^4 P}{{\rm d}\alpha\,{\rm d}\gamma\,{\rm d}\delta\,{\rm d}\log_{10} M}\right|_{\rm obs} \propto \int_0^{\infty} {\rm d}\sigma_8 \left.\frac{{\rm d}^5 P}{{\rm d}\alpha\,{\rm d}\gamma\,{\rm d}\delta\,{\rm d}\log_{10} M\,{\rm d}\sigma_8}\right|_{\rm obs}. \tag{12}$$

The likelihoods in equation (11) for B and β are

$$L_B = {\rm e}^{(-1/2)(B-\bar{B}/\Delta B)^2} \quad \text{and} \quad L_{\beta} = {\rm e}^{(-1/2)[(\beta-\bar{\beta})/\Delta\beta]^2}. \tag{13}$$

In what follows we will consider both the case in which the constraint of the SMBH–halo mass ratio is not included, (so that $L_R = 1$), and the case in which the constraint of the SMBH–halo mass ratio is included. In the later case (which requires an assumption about the SMBH mass ($M_{\rm bh}$), and extrapolation of equation (1) between $z = 0$ and ∼4.8), we have

$$L_R = \int_{-\infty}^{\infty} {\rm d}\log_{10} M_{\rm bh} \frac{{\rm d}P_{\rm prior}}{{\rm d}\log_{10} M_{\rm bh}} {\rm e}^{(-1/2)[(R-\bar{R})/\Delta R]^2}, \quad (14)$$

where we have marginalized over a prior dependence on SMBH mass powering the high-redshift quasars.

2.4 Prior parameter distributions

In this section we specify the prior probability distributions ($P_{\rm prior}$) for parameters under investigation. In cases where parameters are independently constrained we present our representation of the observed distribution ($P_{\rm obs}$).

The value of B is independent of the magnitude of the unknown quasar lifetime. However in addition to the halo mass, the value of B depends on the form of the redshift *evolution* of τ. The z dependence of $t_{\rm q}$ is handled by using the parameter $\alpha_{\rm lt}$. The expected range of $\alpha_{\rm lt}$ may be set by the following considerations. First, if the quasar lifetime is determined by the mass e-fold time-scale of the SMBHs, then $t_{\rm q}$ is independent of redshift, $\tau \propto 1/H^{-1}(z)$ and $\alpha_{\rm lt} \approx 3/2$. Secondly, if the quasar lifetime is determined by the dynamical time-scale at z, then $t_{\rm q} \approx H^{-1}(z)$ making τ independent of redshift and $\alpha_{\rm lt} \simeq 0$. [This is also true if $t_{\rm q} > H^{-1}(z)$.] The evolution of the parameter τ also depends on the evolution of $\epsilon \propto (1+z)^{\alpha_\epsilon}$. We expect the value of ϵ to grow with time, hence $\alpha_\epsilon < 0$. Thus the evolution of τ is parametrized according to $\tau \propto (1+z)^{\alpha}$, where $\alpha = \alpha_{\rm lt} + \alpha_\epsilon$. We take the prior probability for α to be flat over a wide range of values

$$\frac{{\rm d}P_{\rm prior}}{{\rm d}\alpha} = \frac{1}{\alpha_{\rm max} - \alpha_{\rm min}} \quad \text{where} \quad \alpha_{\rm min} = -2, \alpha_{\rm max} = 4. \quad (15)$$

In addition, the value of B depends on the evolution of the relation between luminosity and halo mass (γ). In Paper I we have shown that $\gamma > 0$ under the assumption of constant ϵ, by rejecting the null hypothesis that $\gamma = 0$. There are two components of the parameter γ. First, the SMBH to halo mass ratio can vary with redshift (a dependence described by a parameter $\gamma_{\rm ratio}$). Secondly, the accretion rate could vary with redshift (a dependence which we describe by a parameter $\gamma_{\rm acc}$). Since the accretion rate is close to Eddington at high redshift (Fan et al. 2004), we expect $\gamma_{\rm acc} > 0$. The combined evolution of the quasar luminosity to halo mass ratio may then be described by $\gamma = \gamma_{\rm ratio} + \gamma_{\rm acc}$. Feedback scenarios at constant accretion rate imply $\gamma = 2.5$. We use the following broad prior probability distribution for γ which includes these values.

$$\frac{{\rm d}P_{\rm prior}}{{\rm d}\gamma} = \frac{1}{\gamma_{\rm max} - \gamma_{\rm min}} \quad \text{where} \quad \gamma_{\rm min} = -1, \ \gamma_{\rm max} = 9/2. \quad (16)$$

The value of β is independent of the unknown values of the quasar lifetime (including its evolution α) as well as γ. However in addition to the halo mass, the value of β depends on the form of the relation between quasar luminosity and halo mass (δ). As before there are two components to δ. First, the SMBH to halo mass ratio can vary with halo mass at fixed redshift (a dependence described by a parameter $\delta_{\rm ratio}$). Secondly, the accretion rate at fixed redshift could vary with halo mass (a dependence which we describe by a parameter $\delta_{\rm acc}$). Since the accretion rate is close to Eddington in the most luminous high-redshift quasars (Fan et al. 2004), we expect $\delta_{\rm acc} > 0$. The combined evolution may then be described by $\delta = \delta_{\rm ratio} + \delta_{\rm acc}$. Locally, the SMBH to halo mass relation is steeper than linear ($\delta > 1$), while feedback driven scenarios at constant accretion rate, as well as observation prefer $\delta \sim 4/3$–$5/3$. We consider two cases for prior knowledge of δ. First, we use the following prior, which ignores externally derived constraints

$$\frac{{\rm d}P_{\rm prior}}{{\rm d}\delta} = \frac{1}{\delta_{\rm max} - \delta_{\rm min}} \quad \text{where} \quad \delta_{\rm min} = 1/2, \ \delta_{\rm max} = 5/2. \quad (17)$$

Secondly, we assume that the accretion rate is insensitive to halo mass ($\delta_{\rm acc} = 0$), so that at fixed redshift the SMBH mass depends only on the halo mass. Locally, direct estimates of SMBH and host mass can be made through observations of galaxy dynamics. These observations reveal a correlation between SMBH mass and the characteristic velocity of the surrounding stellar spheroid (e.g. Merritt & Ferrarese 2001; Tremaine et al. 2002), and by extension of the host dark matter halo (Ferrarese 2002). We therefore also consider the case where δ is hypothesized to be redshift independent so that the observed constraint can be applied at high redshift. In this case we take

$$\frac{{\rm d}P_{\rm obs}}{{\rm d}\delta} = \frac{1}{\sqrt{2\pi}\Delta\delta} {\rm e}^{-(1/2)[(\bar{\delta}-\delta)/\Delta\delta]^2}, \quad (18)$$

with a mean and variance of $\bar{\delta} = 1.5$ and $\Delta\delta = 0.25$.

Comparison of the high-redshift SMBH to halo mass ratio with the ratio expected by extrapolating the local value to high redshift requires an assumption about the SMBH mass. SMBHs powering the highest redshift quasars are believed to have masses of $M_{\rm bh} \sim 10^9\,{\rm M}_\odot$ (Fan et al. 2001). We consider the following prior probability for the SMBH mass ($M_{\rm bh}$) powering the high-redshift quasars.

$$\frac{{\rm d}P_{\rm prior}}{{\rm d}\log_{10} M_{\rm bh}} = \frac{1}{\log_{10} M_{\rm bh,max} - \log_{10} M_{\rm bh,min}}, \quad (19)$$

where $\log_{10} M_{\rm bh,min} = 8.5$, $\log_{10} M_{\rm bh,max} = 9.5$.

Of course, all constraints depend on the value of $\log_{10} M$. SMBHs powering the highest redshift quasars are though to have masses in excess of $10^8\,{\rm M}_\odot$, implying halo masses of $M > 10^9\,{\rm M}_\odot$. Galaxies are not observed to have haloes in excess of $10^{14}\,{\rm M}_\odot$. Hence we choose a prior probability for $\log_{10} M$ of the form

$$\frac{{\rm d}P_{\rm prior}}{{\rm d}\log_{10} M} = \frac{1}{\log_{10} M_{\rm max} - \log_{10} M_{\rm min}}, \quad (20)$$

where $\log_{10} M_{\rm min} = 9$, $\log_{10} M_{\rm max} = 14$.

Finally, The evaluation of the PS mass function, and hence of the parameters B and β depend on the adopted cosmology, with the greatest dependence being on σ_8. We utilize the observed distribution for σ_8 from *WMAP* (Spergel et al. 2003)

$$\frac{{\rm d}P_{\rm obs}}{{\rm d}\sigma_8} = \frac{1}{\sqrt{2\pi}\Delta\sigma_8} {\rm e}^{(-1/2)[(\bar{\sigma}_8-\sigma_8)/\Delta\sigma_8]^2}, \quad (21)$$

with mean and variance of $\bar{\sigma}_8 = 0.84$ and $\Delta\sigma_8 = 0.04$.

3 PARAMETER CONSTRAINTS

In this section we present a posteriori, joint probability distributions for combinations of α, γ, δ and $\log_{10} M$. These distributions were obtained by marginalizing equation (12) over the other parameters. For example, the joint probability for γ and $\log_{10} M$ may be found from

$$\frac{{\rm d}^2 P}{{\rm d}\gamma\,{\rm d}\log_{10} M} \propto \int_{-\infty}^{\infty} {\rm d}\alpha \int_{-\infty}^{\infty} {\rm d}\delta \frac{{\rm d}^4 P}{{\rm d}\alpha\,{\rm d}\gamma\,{\rm d}\delta\,{\rm d}\log_{10} M}. \quad (22)$$

We also determine a posteriori cumulative probability distributions for individual parameters. For example, the cumulative probability for $\log_{10} M$ is

$$P(<\log_{10} M) \propto \int_{-\infty}^{\log_{10} M} \mathrm{d}\log_{10} M' \times \int_{-\infty}^{\infty} \mathrm{d}\alpha \int_{-\infty}^{\infty} \mathrm{d}\delta \int_{-\infty}^{\infty} \mathrm{d}\gamma \frac{\mathrm{d}^4 P}{\mathrm{d}\alpha\, \mathrm{d}\gamma\, \mathrm{d}\delta\, \mathrm{d}\log_{10} M'}. \quad (23)$$

We show results in three different cases as follows.

(i) Case I: We begin by determining the constraints that can be made considering only the limits on B and β derived from the SDSS quasars, that is, $L_R = 1$ and assumption only of the prior probability (equation 17) for δ. In this case we are trying to determine four parameters from two constraints, and so are strongly underconstrained.

(ii) Case II: We next determine the constraints that can be made considering the limits on R_0 in addition to those on B and β, thus L_R is given by equation (14). As in Case I, we assume a flat prior probability (equation 17) for δ. The addition of the third constraint partially breaks the degeneracies in Case I.

(iii) Case III: Finally, we replace the prior probability (equation 17) for δ, with the distribution observed locally (equation 18).

Results are presented in Figs 1–3 for Cases I–III, respectively. The sets of panels in the upper two rows show contours of $\mathrm{d}^2P/(\mathrm{d}\alpha\, \mathrm{d}\gamma)|_{\rm obs}$, $\mathrm{d}^2P/(\mathrm{d}\alpha\, \mathrm{d}\delta)|_{\rm obs}$, $\mathrm{d}^2P/(\mathrm{d}\delta\, \mathrm{d}\gamma)|_{\rm obs}$, $\mathrm{d}^2P/(\mathrm{d}\gamma\, \mathrm{d}\log_{10} M)|_{\rm obs}$, $\mathrm{d}^2P/(\mathrm{d}\delta\, \mathrm{d}\log_{10} M)|_{\rm obs}$ and $\mathrm{d}^2P/(\mathrm{d}\alpha\, \mathrm{d}\log_{10} M)|_{\rm obs}$. For the display of joint probability distributions, the solid, dashed, dot–dashed and dotted contours correspond to values that are 0.61, 0.26, 0.14 and 0.036 times the distributions peak value, whose position is marked by a dot. When applied to a Gaussian distribution, these values correspond to the 1, 2, 3 and 5σ levels, respectively. We also show a posteriori cumulative probability distributions for individual parameters in the lower rows of Figs 1–3 (dark lines) together with the corresponding prior probability distributions (light lines).

For each case we determine the values corresponding to the maximum likelihood solution normalized with respect to a maximum possible value of unity. Maximum likelihoods of order unity imply that the model is able to accommodate all constraints simultaneously. The values corresponding to the maximum likelihood solution are shown in Figs 1–3 (large crosses). For Case I the maximum value of the likelihood is given by $L_{\rm I} = L_\beta L_B$. For Case II we include the constraint of local mass ratio so that the likelihood becomes $L_{\rm II} = L_\beta L_B L_R$. Finally, the addition of prior information on the parameter δ leads to a maximum value for the likelihood in Case III of $L_{\rm III} = L_\beta L_B L_R \mathrm{e}^{-1/2[(\bar{\delta}-\delta)/\Delta\delta]^2}$.

We consider each case in turn in the following.

Case I: In the first case we determine what can be learned regarding the connection between SMBHs and host haloes, using only the evolution in the number counts of quasars at high redshift and the slope of the high-redshift quasar luminosity function. The results are shown in Fig. 1. In this case we have two parameters that may

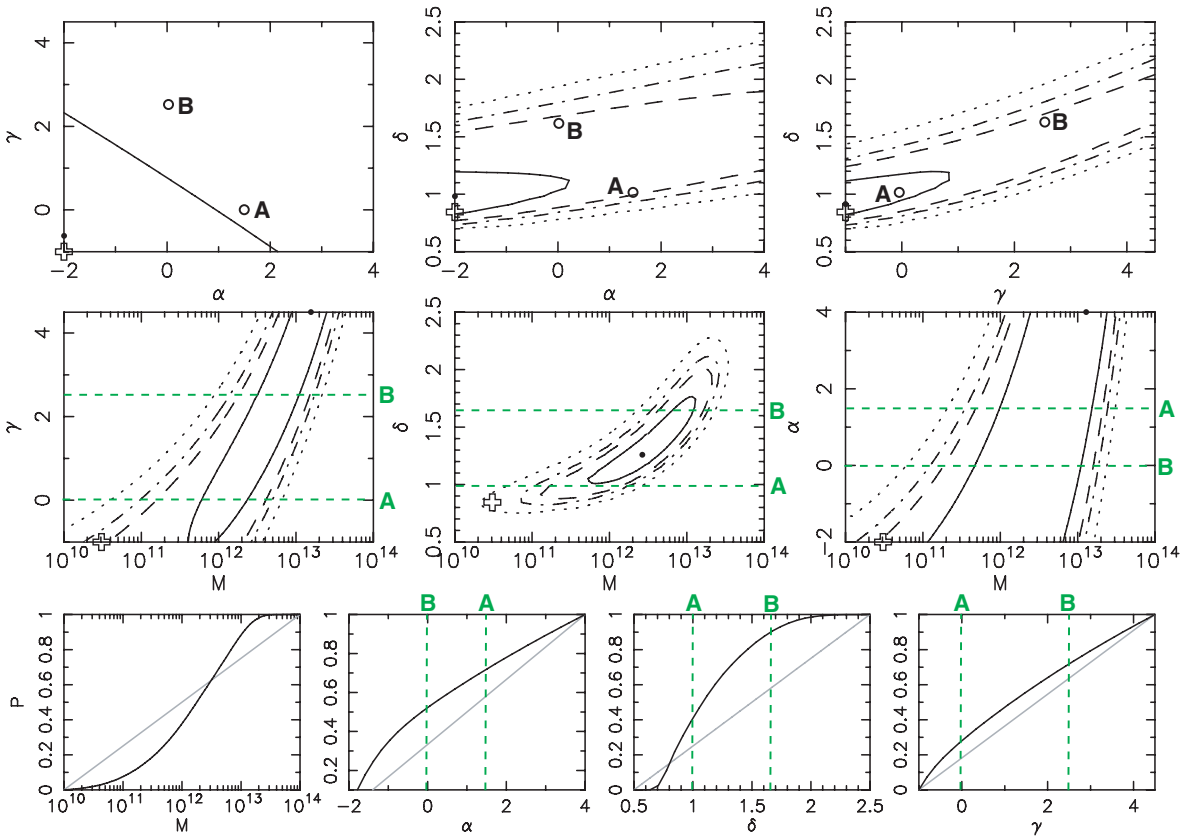

Figure 1. Constraints on power-law parameters, Case I: the various panels in the upper two rows show contours for the marginalized a posteriori joint probability distributions for combinations of the parameters γ, δ, α and M. The dots show the location of the maximum likelihood within the marginalized distributions, while the cross shows the location of the maximum likelihood within the full four-dimensional parameter space. The lower row shows marginalized a posteriori cumulative probability distributions for γ, δ, α and M (dark lines). The light lines show the respective prior probability distributions. The large open circles in the upper panels, and the light dashed lines in the central and lower panels show the location in parameter space of models A and B described in Section 7.

be measured (β and B) but four model parameters that lack prior constraints. Clearly this problem is underconstrained. Inspection of equations (7) and (9) shows that β depends only on M and δ, while B is a function of all four parameters. Thus we would expect a degeneracy in the determination of parameters δ and M which is driven by the observed luminosity function slope β. This degeneracy is clearly seen in the middle panel of Fig. 1, although it is broken at high and at low M by the additional constraints from B. Thus even in this underconstrained case we are able to obtain an estimate of mass, and show that $\delta > 1$. The preferred value for the parameter δ is quite insensitive to the value of either α or γ. Because the measured value of B is degenerate between M (or δ through the constraint of β), γ and α, there will be a degeneracy along a line in the three dimensional parameter space. As a result we see that no constraints are possible in the γ–α plane, while there are strong degeneracies between α and M and between γ and M. The maximum value of the likelihood is $L_{\rm I} = 0.92$, implying that the best-fitting model is a very good fit to the high-redshift data. The set of best-fitting parameters is $(\log_{10} M, \gamma, \delta, \alpha) = (10.48, -1, 0.84, -2)$. The best-fitting value of α is on the edge of the range of parameter space, which is indicative of the degeneracies between α and other parameters.

Parameters for which the data are the restrictive have a posteriori probability distributions that differ from the assumed prior-probability distributions. As a result the lack of restriction imposed on models for SMBH growth by the high-redshift luminosity function may be clearly seen in the lower row of Fig. 1. While the high-redshift luminosity function places limits on each of the parameters δ and M, no limits may be placed on the parameters α or γ. Additional observables must therefore be included in order to constrain the models. We next turn to inclusion of the likelihood based on the local SMBH to halo mass ratio.

Case II: We can break part of the degeneracy seen in Case I by including the likelihood for the local SMBH to halo mass ratio (equation 14) as an additional constraint. This inclusion has a two-fold effect on the parameter fit. First, it couples the dependence of the overall likelihood of a solution on δ and γ in a direct way. The likelihood for the ratio R will therefore be degenerate between δ and γ. Secondly, the value of γ is now constrained by the likelihood for R in addition to the likelihood for B. This breaks the three-way degeneracy between M, α and γ. The interplay between the different likelihoods and parameters is now coupled so that simple interpretation of the solution is more difficult than in Case I. However, we now have three observables (B, β and R), from which to constrain four parameters. The solution must therefore still be subject to a certain degree of degeneracy.

The results are shown in Fig. 2. We find that the combinations of γ with M, δ with M and γ with δ are well constrained. In particular we find $\gamma > 0$. This may also be seen by inspecting the a posteriori cumulative probability distributions. We see that γ, δ and $\log_{10} M$ have a posteriori distributions that differ substantially from their prior probabilities, indicating that the data are able to constrain their values. The value of δ lies between 1.1 and 1.6 (90 per cent), and is

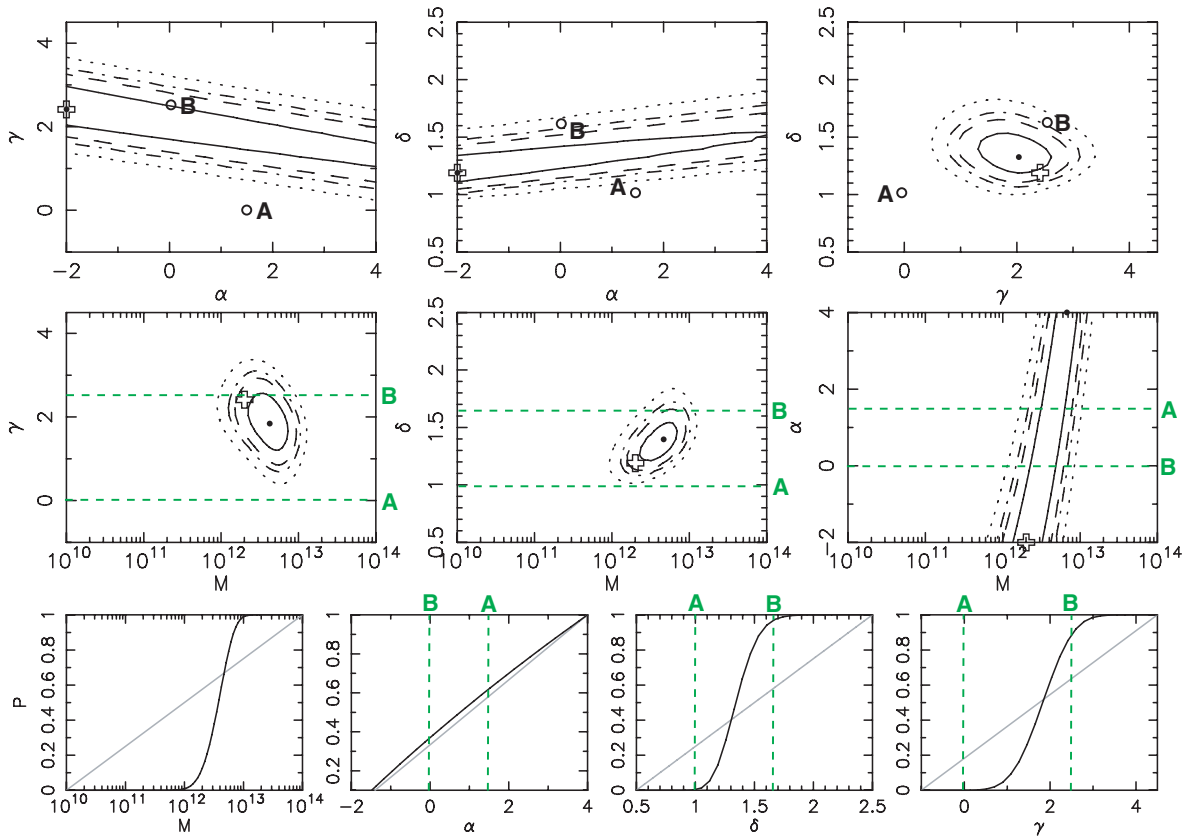

Figure 2. Constraints on power-law parameters, Case II: the various panels in the upper two rows show contours for the marginalized a posteriori joint probability distributions for combinations of the parameters γ, δ, α and M. The dots show the location of the maximum likelihood within the marginalized distributions, while the cross shows the location of the maximum likelihood within the full four-dimensional parameter space. The lower row shows marginalized a posteriori cumulative probability distributions for γ, δ, α and M (dark lines). The light lines show the respective prior probability distributions. The large open circles in the upper panels, and the light dashed lines in the central and lower panels show the location in parameter space of models A and B described in Section 7.

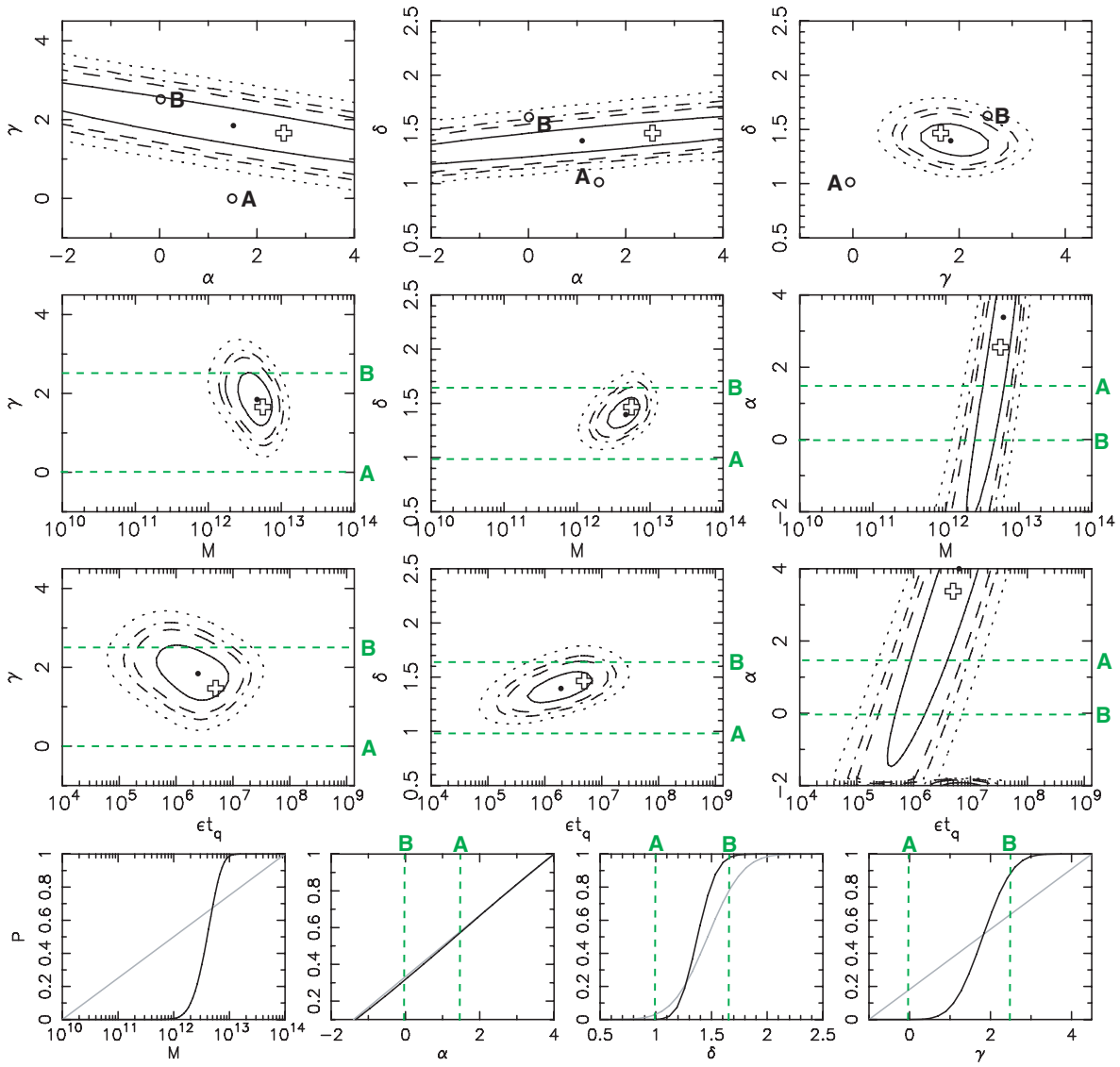

Figure 3. Constraints on power-law parameters, Case III: the upper and second rows show contours for the marginalized a posteriori joint probability distributions for combinations of the parameters γ, δ, α and M. The third row shows distributions with M replaced by $(\epsilon t_{\rm lt})$. The dots show the location of the maximum likelihood within the marginalized distributions, while the cross shows the location of the maximum likelihood within the full four-dimensional parameter space. The lower row shows marginalized a posteriori cumulative probability distributions for γ, δ, α and M (dark lines). The light lines show the respective prior probability distributions. The large open circles in the upper panels, and the light dashed lines in the panels of the second, third and lower rows show the location in parameter space of models A and B described in Section 7.

larger than unity in agreement with the locally observed prior probability distribution for δ that will be included in Case III. The mass is constrained to be larger than $10^{12.2}\,{\rm M}_\odot$ and smaller than $10^{12.8}\,{\rm M}_\odot$ (90 per cent), while $1 < \gamma < 2.7$ (90 per cent). Unless the accretion rate is changing rapidly with redshift near $z \sim 4.5$, the positive value of γ implies an SMBH to halo mass ratio that decreases with time. The main degeneracies due to the remaining degree of freedom are between α and M (lower right-hand panel), between α and δ (upper middle) and between α and γ (upper left-hand panel), although the dependencies on α are weak. The maximum value of the likelihood is $L_{\rm II} = 0.48$, implying that the best-fitting model remains a very good fit to the data following the addition of the constraint on the mass ratio. The set of best-fitting parameters is $(\log_{10} M, \gamma, \delta, \alpha) = (12.3, 2.41, 1.19, -2.)$. The value of α remains at the edge of the range of parameter space, indicating that the degeneracies between α and other parameters is not removed through the inclusion of the mass ratio.

Case III: Finally, we include a prior probability for δ (equation 18) based on observations of SMBHs at low redshift. The results are plotted in the upper and central rows of Fig. 3. Strictly speaking the solution is still underconstrained since there are four parameters and three constraints. However, the observed prior distribution for δ is sufficiently narrow that the hypothesis of the slope in the local relation (δ) also holding at high redshift strongly constrains the solution. The result is that both γ and M are tightly constrained by the data. The maximum likelihood value is $L_{\rm III} = 0.40$, with a set of best-fitting parameters $(\log_{10} M, \gamma, \delta, \alpha) = (12.7, 1.65, 1.47, 2.55)$. From the lower row of Fig. 3 we see that only γ and $\log_{10} M$ have a posteriori distributions that differ substantially from their prior probabilities. The data do not restrict δ much beyond the assumed prior

probability in this case. However, this indicates that the preferred value of δ at $z \sim 4.5$ is similar to the local value as hypothesized. As in Case II the data show a definite preferred solution for these quantities. SMBHs form a smaller fraction of their hosts mass at early times than they do today, $1 < \gamma < 2.8$ (90 per cent), with high-redshift host masses of $10^{12.2-12.8}\,\mathrm{M}_\odot$ (90 per cent). The parameter α remains unconstrained.

4 QUASAR LIFETIME

If a fraction ϵ of dark matter haloes contain SMBHs, then the total lifetime of the quasar can be estimated (Haiman & Hui 2001; Martini & Weinberg 2001) by dividing the quasar density $\Psi(\mathcal{M}_{1450} < -26.7, z)$ by ϵ times the density $N(>M)$ of haloes larger than M, and then multiplying by the Hubble time (for $t_\mathrm{q} < H^{-1}$), hence

$$\epsilon t_\mathrm{q}(\Psi, M) = H^{-1}(z)\frac{\Psi(z)}{N(>M, z)}. \quad (24)$$

There is therefore a one to one correspondence between ϵt_q and M. As a result the joint a posteriori distribution, with M replaced by ϵt_q may be obtained as

$$\left.\frac{\mathrm{d}^4 P}{\mathrm{d}\alpha\,\mathrm{d}\gamma\,\mathrm{d}\delta\,\mathrm{d}\log_{10}(\epsilon t_\mathrm{q})}\right|_\mathrm{obs} \propto \int \mathrm{d}\sigma_8 \frac{\mathrm{d}P_\mathrm{prior}}{\mathrm{d}\sigma_8}\left.\frac{\mathrm{d}^5 P}{\mathrm{d}\alpha\,\mathrm{d}\gamma\,\mathrm{d}\delta\,\mathrm{d}\log_{10} M\,\mathrm{d}\sigma_8}\right|_\mathrm{obs}\frac{\mathrm{d}\log_{10} M}{\mathrm{d}\log_{10}(\epsilon t_\mathrm{q})}, \quad (25)$$

where

$$\frac{\mathrm{d}\log_{10} M}{\mathrm{d}\log_{10}(\epsilon t_\mathrm{q})} = \left[\frac{d}{\mathrm{d}\log_{10} M}\int \mathrm{d}\Psi \frac{dP}{\mathrm{d}\Psi}\epsilon t_\mathrm{q}(\Psi, M)\right]^{-1}. \quad (26)$$

In the third row of Fig. 3 we show the joint probability distributions (computed using equation 25) for α and $\log_{10}(\epsilon t_\mathrm{q})$, γ and $\log_{10}(\epsilon t_\mathrm{q})$, and for δ and $\log_{10}(\epsilon t_\mathrm{q})$. The distributions were computed using Case III constraints. The behaviour is similar to that for the distributions of $\log_{10} M$ as expected. If the occupation fraction is of order unity, then we find lifetimes of 10^{6-7} yr, in agreement with estimates at lower redshifts. Observed quasar lifetimes therefore suggest an occupation fraction ϵ that is of order unity. Since the Hubble time is $\sim 10^9$ yr at $z \sim 4.8$, we find that the occupation fraction must be larger than $\epsilon \sim 10^{-3}$ to 10^{-2}.

5 SCATTER IN THE LUMINOSITY–HALO MASS RELATION

Up till now we have assumed a one-to-one correspondence between halo mass and quasar luminosity (equation 1). However, we would expect a scatter in this relation, due to (at least because of) scatter in the M_bh–M relation, and due to variation in the accretion rate. To assess the importance of this scatter, we make the following modification to the calculation already described. We have associated a quasar of luminosity L with a halo of mass M. We can regard the mass M as characteristic, and replace the density of haloes $n(M, z)$ with an effective density

$$n_\mathrm{eff}(M, z) = \frac{1}{\sqrt{2\pi}\Delta m}\int_0^\infty \mathrm{d}m' n(M', z)\mathrm{e}^{(-1/2)[(m'-m)/\Delta m]^2}, \quad (27)$$

which is obtained as a weighted average of the densities of haloes that house a quasar of luminosity L. Here $m \equiv \log_{10} M$. Effective values of B, γ, etc. can then be calculated using $n_\mathrm{eff}(M, z)$. We have computed the resulting probability distributions for α, γ, δ and $\log_{10} M$ as before in order to assess the importance of scatter in equation (1). Distributions corresponding to Case III were computed taking $\Delta m = 0.5$ (so that 68 per cent of haloes are contained within one decade of mass), and are plotted in Fig. 4.

The results are similar to those obtained in the absence of scatter. In particular the contours for distributions move by less than 1-sigma, and have quantitatively similar values. The maximum value of the likelihood is $L_\mathrm{III} = 0.38$, implying that the best-fitting model remains a very good fit to the data following the addition of scatter in the SMBH–halo mass relation. The set of best-fitting parameters is $(\log_{10} M, \gamma, \delta, \alpha) = (12.62, 1.84, 1.47, 3.59)$.

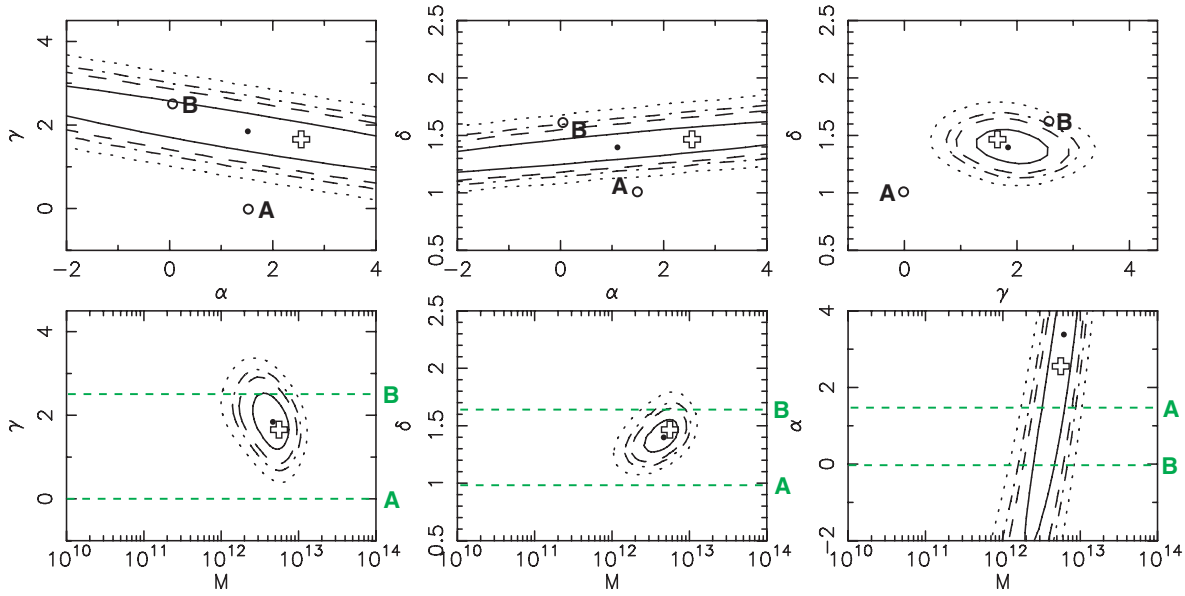

Figure 4. Constraints on power-law parameters where scatter in the SMBH to halo mass ratio is included, Case III: the various panels show contours for the marginalized a posteriori joint probability distributions for combinations of the parameters γ, δ, α and M. The dots show the location of the maximum likelihood within the marginalized distributions, while the cross shows the location of the maximum likelihood within the full four-dimensional parameter space. The large open circles in the upper panels, and the light dashed lines in the lower panels show the location in parameter space of models A and B described in Section 7.

6 DEPENDENCE OF RESULTS ON CHOICE OF PRIORS AND PARAMETRIZATION

In this paper our aim is to determine what physical properties may be inferred from the high-redshift quasar luminosity function within a general, rather than a specific framework. Two issues arise regarding the statistical robustness of our results. First, having chosen a particular parametrization for our model we then calculate likelihoods for parameters using that parametrization (e.g. $\log_{10} M, \gamma$ and α in our prescription). We have chosen flat prior probability distributions for these parameters and hence find a posteriori probabilities for their values. Now if the observations are able to genuinely constrain the values of these parameters, then our results should be independent of the prior used (within reason). We would therefore like to know whether our results are sensitive to the choice of prior. Secondly, we have chosen a power-law parametrization for the redshift dependencies of the lifetime and SMBH to halo mass ratio. These parametrizations may or not provide an adequate description of reality. We would therefore like to know whether the choice of parametrization affects our physical conclusions regarding the mass of host dark matter haloes, or the evolution of the SMBH to halo mass ratio. We discuss these issues in the remainder of this section.

6.1 Dependence on prior probabilities

Up till now we have assumed prior probability distributions for dimensionless parameters (α, γ and δ) that are flat (i.e. $\mathrm{d}P_{\rm prior}/\mathrm{d}\alpha \propto 1$ etc.). For the dimensioned quantity (M) we have assumed a prior probability that is flat in the logarithm [i.e. $\mathrm{d}P_{\rm prior}/\mathrm{d}\log_{10}(M) \propto 1$]. While these are the natural choices, we have repeated the calculations in Case II assuming priors for γ and δ that are flat in the logarithm (for $0 < \gamma < 9/2$ and $1/2 < \delta < 5/2$), and a prior probability $\mathrm{d}P_{\rm prior}/\mathrm{d}M \propto 1$, where $10^9\,\mathrm{M}_\odot < M < 10^{14}\,\mathrm{M}_\odot$ for host halo mass. We have not changed the prior of the unconstrained parameter α.

Fig. 5 shows the resulting parameter constraints. The set of best-fitting parameters is $(\log_{10} M, \gamma, \delta, \alpha) = (12.87, 1.08, 1.47, 4.0)$. The constrained value for M is quite similar to the original case (Fig. 2), thus the estimate of this (physical) parameter would appear to be insensitive to the choice of prior. The values of δ and γ also take similar values indicating that they are constrained by the data rather than by the prior. The conclusion that the SMBH to halo mass ratio was larger in the past ($\gamma > 0$) is therefore not sensitive to the choice of prior. The value of α remains the least constrained, although positive values are preferred in this case.

6.2 Exponential parameter constraints

The parameters α and γ describe redshift dependencies of the lifetime and SMBH to halo mass ratio, respectively. Up till now we have specified power-law evolutions for these quantities, and constrained the allowed values of the corresponding parameters. Of course it is only our theoretical prejudice that leads us to specify a power law, since we have no observational evidence for this form of parametrization. The assumption of a particular prior probability distribution for a parameter (Bayes postulate) leads to prior probabilities for the physical parameter of interest (like the lifetime or mass ratio) that depend on the parametrization employed. We would therefore like to check that our choice of model does not qualitatively bias the results. To check the effect of our choice of parametrization, we have re-calculated our results assuming exponential rather than power-law evolution for those quantities that vary with redshift (i.e. τ and $L(z)/L_0$). However, we retain our power-law form for mass ratio at fixed redshift (δ) since this is an observed rather than a postulated parametrization.

Thus equations (1) and (5) become

$$\frac{L(z)}{L_0} = \frac{M_{\rm bh}(z)}{M_{\rm bh,0}} = \left(\frac{M}{M_0}\right)^{\delta} \mathrm{e}^{\gamma z} \tag{28}$$

and

$$\frac{\tau(z)}{\tau_0} = \mathrm{e}^{\alpha z}, \tag{29}$$

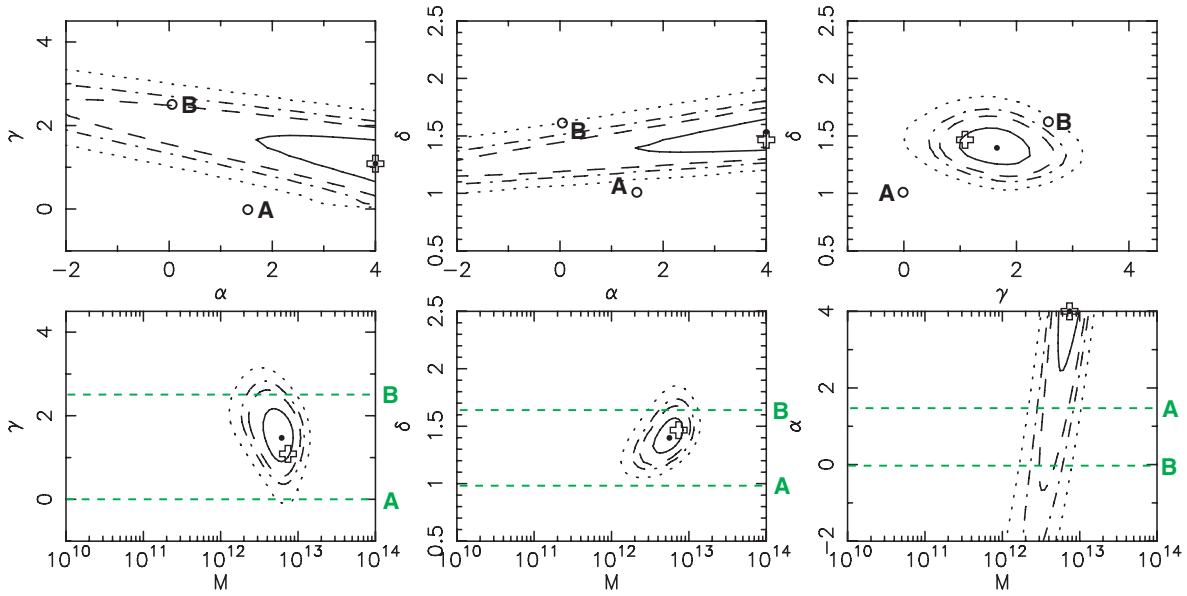

Figure 5. Constraints on power-law parameters assuming alternative priors, Case II: the various panels show contours for the marginalized a posteriori joint probability distributions for combinations of the parameters γ, δ, α and M. The dots show the location of the maximum likelihood within the marginalized distributions, while the cross shows the location of the maximum likelihood within the full four-dimensional parameter space.

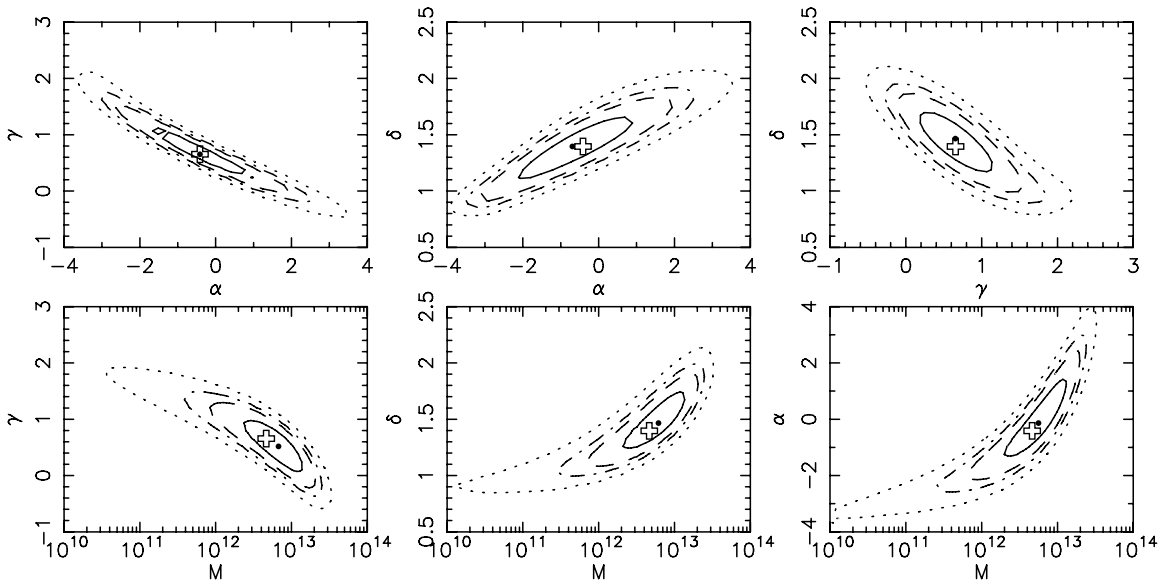

Figure 6. Constraints on power-law (δ) and exponential (α and γ) parameters, Case III: the various panels show contours for the marginalized a posteriori joint probability distributions for combinations of the parameters γ, δ, α and M. The dots show the location of the maximum likelihood within the marginalized distributions, while the cross shows the location of the maximum likelihood within the full four-dimensional parameter space.

which leads to evolution described by the equation

$$B = 0.434\alpha + \frac{\partial \log_{10} N(>M, z)}{\partial z} + 0.434\gamma \frac{\mathrm{d} \log_{10} N(>M, z)}{\mathrm{d} \log_{10} M}. \quad (30)$$

The constraint from the local mass ratio (equation 10) becomes

$$R_0\left(10^{12}\,\mathrm{M}_\odot, 0\right) = R\,(M, z)\left(\frac{M}{10^{12}\,\mathrm{M}_\odot}\right)^{1-\delta} \mathrm{e}^{-\gamma z}, \quad (31)$$

while the constraint based on the slope of the luminosity function (equation 9) remains unchanged. Note that the relation of B to R as a function of γ is altered by the new definition.

Fig. 6 shows the resulting parameter constraints assuming the analysis described in Case III. The constrained value for M is quite similar to the power-law case (Fig. 3), thus the estimate of this (physical) parameter would appear to be insensitive to the choice of parametrization (assuming a monotonic evolution over the range of interest). The maximum value of the likelihood is $L_{\mathrm{III}} = 0.43$, implying that the best-fitting exponential model also provides a very good fit to the data. The set of best-fitting parameters is $(\log_{10} M, \gamma, \delta, \alpha) = (12.7, 0.66, 1.4, -0.41)$. The values of α and γ will clearly differ from the power-law case. However, the conclusion that the SMBH to halo mass ratio was larger in the past ($\gamma > 0$) holds in the exponential case as in the power-law case. The exponential parametrization allows a preferred value of $\alpha \sim 0$, indicating an occupation fraction and/or duty cycle that does not vary much with redshift.

7 COMPARISON WITH SIMPLE PHYSICAL MODELS

Before concluding, we apply our idea to a couple of simple test case models. Among the successful models of the high-redshift quasar luminosity function, two examples employ particularly simple but different physical hypotheses. In the first, the quasar lifetime is constant (perhaps set by the Salpeter time) with an occupation fraction of unity, the SMBH makes up a constant fraction of the host halo mass, and the quasar shines at its Eddington rate (Haehnelt et al. 1998; Haiman & Loeb 1998). We refer to this as model A. In the second model, the SMBH mass is set by feedback (through energy conservation) over the dynamical time of the gas reservoir, the occupation fraction is of order unity and the quasar shines at its Eddington rate (Haehnelt et al. 1998; Silk & Rees 1998; Wyithe & Loeb 2003). We refer to this as model B. In the present context these two models may be described by the parameter sets $(\alpha_{\mathrm{A}}, \gamma_{\mathrm{A}}, \delta_{\mathrm{A}}) = (1.5, 0, 1)$ and $(\alpha_{\mathrm{B}}, \gamma_{\mathrm{B}}, \delta_{\mathrm{B}}) = (0, 2.5, 1.66)$, respectively. The locations of these models in parameter space are shown in Figs 1–5 by the light dashed lines, and the letters {A} and {B}.

Considering first the constraints in Case I (Fig. 1), we see that the degeneracies prohibit any conclusion regarding α or γ, while the preferred δ lies between the two models. Indeed the two models may not be distinguished at all based on the luminosity function data alone. On the other hand the simple models described should also be able to accommodate the constraint from the local SMBH to halo mass ratio. In Case II (Figs 2 and 5) the different values of α for the two models are again indistinguishable. However, in contrast the values of γ and δ are more consistent with the feedback driven model (model B). Finally, if the prior probability for δ is included (Case III, Figs 3–4) then we have ruled out 'model A' a priori. However, in this final case it is still instructive to investigate the consistency of model B with observation. The model B values of $\delta_{\mathrm{B}} = 1.66$ and $\gamma_{\mathrm{B}} = 2.5$ are consistent with the data.

These results suggest that model B is more consistent with the data than model A. However, it is interesting to note that the most likely values for the parameters γ and δ lie between those of the two models, indicating that neither describes the astrophysics in its totality. On the other hand, Fig. 3 demonstrates in a model independent way, that the data would prefer an SMBH to halo mass ratio that is larger at higher redshifts (as suggested by the evolution of the virial-mass–virial velocity relation), combined with an SMBH to halo mass ratio that is larger in higher mass haloes. These conclusions are insensitive to the addition of scatter in the luminosity–halo

mass relation, to the form of parametrization, and to the prior probabilities assumed.

8 SUMMARY

In this paper we have investigated the constraints that observations of the high-redshift luminosity function place on SMBH evolution. Our approach differs from that traditionally employed. Rather than hypothesize a physical model to govern the formation and evolution of SMBHs, we have described a general parametrized model and determined the regions of the resulting parameter space that are admitted by the observations. The traditional approach allows one to demonstrate that a particular model is viable, but does not provide a test of its uniqueness, nor which aspects of the theory are constrained by the data. Conversely our approach explicitly demonstrates the degeneracies among the evolution of different physical properties, and thus reveals which conclusions may be robustly drawn from the data.

We find that in isolation, the available data for the luminosity function of high-redshift quasars is unable to distinguish between a range of different physical models due to a series of degeneracies between different physical properties. The inclusion of the local SMBH to halo mass ratio as a constraint removes some of this degeneracy and allows us to determine the physical parameters that may most clearly be derived from the data. We find that the mass of the high-redshift quasar host haloes was $M = 10^{12.5\pm0.3}\,\mathrm{M}_{\odot}$ (90 per cent). The ratio of SMBH to halo mass was larger at high redshift with a dependence $M_{\rm bh} \propto M(1+z)^{(1.9\pm0.9)}$ [or $M_{\rm bh} \propto Me^{(0.7\pm0.5)z}$] (90 per cent). In addition, the ratio of quasar luminosity to halo mass increases with halo mass. We find $L \propto M^{1.4\pm0.25}$ (90 per cent). In the instance of an accretion rate that is insensitive to halo mass this relation is in agreement with that observed in the local Universe. In hindsight the latter result might have been expected since the PS mass function declines exponentially towards high redshift, while quasar number counts are observed to decline only as a power law. These conclusions are not sensitive to scatter in the relation of SMBH to halo mass, or to the choices of parametrization or prior probabilities, and so must be implicit in any physical model developed to describe SMBH evolution. However, the evolution of lifetime and occupation fraction are not currently probed by the data.

In future, the analysis described in this paper will be enhanced by additional constraints. For example, a larger sample of quasars would allow the slope of the luminosity function β and the evolution of quasar density B to be determined over a range of redshifts. These additional constraints should break some of the remaining degeneracies and provide us with constraints on the evolution of quasar lifetime to go beside the current constraints available for the host halo mass.

ACKNOWLEDGMENTS

The authors thank Zoltan Haiman for helpful comments on a draft of this manuscript. The work of JSBW was supported by the Australian Research Council. This work was initiated when one of the authors (TP) was visiting the School of Physics, University of Melbourne, under the Miegunyah Distinguished Fellowship.

REFERENCES

Bardeen J. M., Bond J. R., Kaiser N., Szalay A. S., 1986, ApJ, 304, 15
Di Matteo T., Croft R. A. C., Springel V., Hernquist L., 2003, ApJ, 593, 56
Efstathiou G., Rees M. J., 1998, MNRAS, 230, 5
Fan X. et al., 2001, AJ, 122, 2833
Fan X. et al., 2003, AJ, 125, 1649
Fan X. et al., 2004, AJ, 128, 515
Ferrarese L., 2002, ApJ, 587, 90
Haehnelt M. G., Natarajan P., Rees M. J., 1998, MNRAS, 300, 817
Haiman Z., Hui L., 2001, ApJ, 547, 27
Haiman Z., Loeb A., 1998, ApJ, 503, 505
Kauffmann G., Haehnelt M. G., 2000, MNRAS, 311, 576
Martini P., Weinberg D. H., 2001, ApJ, 547, 12
Merloni A., Rudnick G., Di Matteo T., 2004, MNRAS, 354, L37
Merritt D., Ferrarese L., 2001, ApJ, 547, 140
Peng C. Y., Impey C. D., Rix H.-W., Kochanek C. S., Keeton C. R., Falco E. E., Lehar J., McLeod B. A., 2006, ApJ, 640, 114
Press W. H., Schechter P., 1974, ApJ, 187, 425
Scannapieco E., Oh S. P., 2004, ApJ, 608, 62
Sheth R., Torman G., 2002, MNRAS, 321, 61
Shields G. A., Menezes K. L., Massart C. A., van den Bout P., 2006, ApJ, 641, 683
Silk J., Rees M. J., 1998, A&A, 331, L1
Spergel D. N. et al., 2003, AJ, 148, 175 (Suppl.)
Tremaine S. et al., 2002, ApJ, 574, 740
Volonteri M., Haardt F., Madau P., 2003, ApJ, 582, 559
Wyithe J. S. B., Loeb A., 2003, ApJ, 595, 614
Wyithe J. S. B., Padmanabhan T., 2006, MNRAS, 366, 1029 (Paper I)

This paper has been typeset from a TEX/LATEX file prepared by the author.